Available online at www.sciencedirect.com

SciVerse ScienceDirect

Ceramics International 39 (2013) S605–S609

CERAMICS INTERNATIONAL

www.elsevier.com/locate/ceramint

Effects of buffer layers on properties of bulk hetero junction flexible organic solar cells

Kun Ho Kim, Ho Jung Chang*

Department of Electronics Engineering, Dankook University, Cheonan-si 330-714, Chungnam, South Korea

Available online 22 October 2012

Abstract

We fabricated the flexible organic solar cells (OSCs) using the alternating co-polymer, poly[*N*-9″-hepta-decanyl-2,7-carbazole-alt-5,5-(4′,7′-di-2-thienyl-2′,1′,3′-benzothiadiazole) (PCDTBT) in bulk hetero junction composites with the fullerene derivative [6,6]-phenyl C_{61}-butyric acid methyl ester (PCBM) active layer for the electron donor and acceptor materials, respectively. The active layer was spin-coated onto various substrates with different buffer layers of lithium fluoride (LiF) and poly(3,4-ethylenedioxythiophene):poly(styrenesulfonate) (PEDOT:PSS) on the indium tin oxide (ITO) coated polyethylene naphthalene (PEN) substrates, such as PEN/ITO/LiF, PEN/ITO/PEDOT:PSS and PEN/ITO/PEDOT:PSS/LiF. The effects of the buffer layer position on the electrical and morphological properties of the devices were investigated. The performance of OSCs coated on the PEN/ITO/PEDOT:PSS/LiF substrate exhibited the best electrical property among the prepared samples, showing the maximum short circuit current, open circuit voltage, fill factor and power conversion efficiency values were about 11.4 mA/cm^2, 0.90 V, 39.3 % and 4.0 %, respectively.

Keywords: A. Films; C. Electrical properties; B. Surfaces; Flexible organic solar cell

1. Introduction

Organic solar cells (OSCs) have attracted a great deal of attention as one of the promising future energy saving devices because of many advantages, such as a flexibility potential, low cost, light weight and large area applications [1–6]. Until now, OSCs have relatively low power conversion efficiency (PCE) with 9.2 % [7] as compared with Si-based inorganic solar cells. In order to improve the PCE value, it would be desirable to optimize the introduced organic materials as well as the device structure of OSCs. As the one way to improve the efficiency of the device, a buffer layer is introduced between electrode and active layer. The efficiency of OSC can be improved when spin-coated with poly(3,4-ethylenedioxythiophene):poly(styrenesulfonate) (PEDOT:PSS) as the buffer layer between indium tin oxide (ITO) and active layer. PEDOT:PSS layer may be not only very effective but also useful to modify the interface between ITO and active layer. However, the interface between PEDOT:PSS and active layer is not stable and the chemical reaction between PEDOT:PSS and active layer can result in degraded device performance [8,9]. In addition, lithium fluoride (LiF) and molybdenum oxide (MoO_3) are also considered as buffer layer materials to improve the performance of device [10,11]. In this study, the OSCs using a poly[*N*-9″-hepta-decanyl-2,7-carbazole-alt-5,5-(4′,7′-di-2-thienyl-2′,1′,3′-benzothiadiazole) (PCDTBT) as the electron donor and fullerene derivative [6,6]-phenyl C_{61}-butyric acid methyl ester (PCBM) as the electron acceptor were prepared by spin coating method onto various flexible polyethylene naphthalene (PEN) substrates with different buffer layers, such as PEN/ITO/LiF, PEN/ITO/PEDOT:PSS and PEN/ITO/PEDOT:PSS/LiF. The PEDOT:PSS and LiF buffer layers were introduced between the ITO electrode and PCDTBT:PCBM bulk hetero-junction active layer. The effects of buffer layers on the electrical and morphological properties of the devices were investigated, and their performances compared for the optimization of the cell structure.

2. Material and methods

Fig. 1(a) shows the molecular structures of PCDTBT and PCBM, which act as the electron donor and acceptor

*Corresponding author. Tel.: +82 41 550 3569; fax: +82 41 550 3589.
E-mail address: hjchang@dankook.ac.kr (H.J. Chang).

0272-8842/$ - see front matter © 2012 Elsevier Ltd and Techna Group S.r.l. All rights reserved.
http://dx.doi.org/10.1016/j.ceramint.2012.10.145

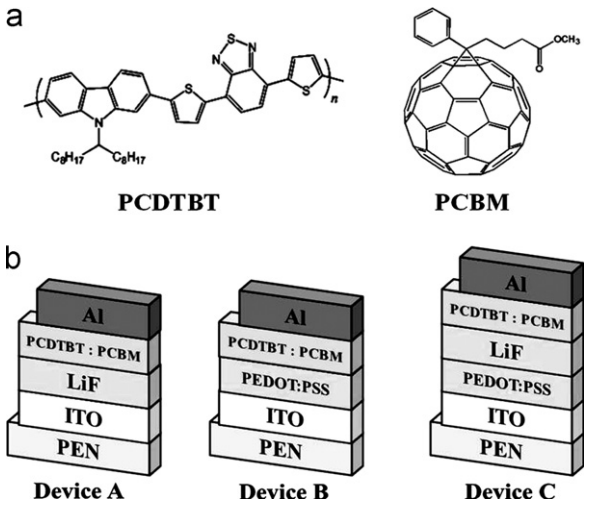

Fig. 1. Molecular structures (a) of PCDTBT and PCBM and (b) the structures of OSCs with three different buffer layers (Devices A–C).

in the active layer. The structures of OSCs with three different buffer layers are shown in Fig. 1(b). In order to fabricate the flexible OSCs with different buffer layers, ITO coated PEN substrates were cleaned with acetone, methanol, and isopropyl alcohol for 5 min in an ultrasonic bath. The ITO anode film with the sheet resistance of 15 Ω/sq was patterned using a conventional photolithography method. And then, a plasma treatment was carried out in order to improve the adhesion between the ITO and the buffer layer (LiF and PEDOT:PSS) as well as to improve the electrical properties of the anode film. The plasma treatment was performed at 150 W radio frequency power for 90 s under an O_2:Ar mixing gas ratio of 2:1 with a pressure of 20 mTorr. The PEDOT:PSS (Baytron P AI4083) precursor solution, used as the hole transport buffer layer, was spin-coated at 5000 rpm for 60 s after being filtered by passing it through a 0.45 μm filter. Then, the substrate was dried at 140 °C for 10 min on a hot plate. The LiF layer was deposited onto the ITO and PEDOT:PSS films by the thermal evaporation method. For preparation of PCDTBT and PCBM precursor solutions, PCDTBT and PCBM powders were combined with concentration ratio of 1:4 wt% and dissolved using dichlorobenzene on a hot plate at 60 °C for 12 h. The prepared PCDTBT:PCDTBT solutions were spin-coated at 700 rpm for 60 s. The film thicknesses of PEDOT:PSS and the PCDTBT:PCBM active layers were found to be about 30 nm and 80 nm, respectively. Finally, the Al cathode layer with thicknesses of 150 nm was deposited using a thermal evaporation method in a vacuum chamber with a base pressure of 5×10^{-8} Torr. The actual active area was about 0.04 cm^2.

In order to investigate the dependence of the buffer layers on the properties of devices, we prepared the flexible OSC samples with different buffer layers such as PEN/ITO/LiF (Device A), PEN/ITO/PEDOT:PSS (Device B), and PEN/ITO/PEDOT:PSS/LiF (Device C). The short circuit current density (J_{SC}) *versus* the open circuit voltage (V_{OC}) characteristics of the devices were measured using a solar simulation measurement system (Newport) under an air mass 1.5G solar irradiation energy (100 mW/cm^2). The light absorption spectrum was measured with a UV–visible spectrophotometer, and an atomic force microscope (AFM, model XE-150) was used to investigate the surface morphology of the film layers with calculated RMS (root-mean-square) values. The contact angle measurement system (model DAS 100) was used to determine the contact angles and surface energy on the buffer layer films using deionized (D.I) water droplets at the temperature of 20 °C with volume of 20 μL.

3. Results and discussion

Fig. 2 demonstrates the intensities of the light absorption spectra of the PCDTBT:PCBM active layers spin-coated on the three kinds of devices (Devices A–C). It was observed that the PCDTBT:PCBM active layer prepared on Device C exhibited the highest light absorption intensity at the wavelengths around 410 nm and 550nm, compared to Device A (without the PEDOT:PSS buffer layer). This result reflects that the optical properties of the active layer are affected by the PEDOT:PSS hole transport buffer layer, suggesting that a large number of photons can be absorbed in the PEDOT:PSS film layer. The OSC device without buffer layers on the ITO/PEN substrate (PEN/ITO/PCDTBT:PCBM structure) showed a similar light absorption pattern with Device A. The surface roughness of the buffer layer may affect the optical and electrical properties of the OSCs. Therefore, we investigated the effects of the surface morphology for the different buffer layers (Devices A–C) on the properties of the OSCs by the AFM measurement.

Fig. 3 represents the AFM surface morphologies for Devices A–C prepared using the different buffer layers. The RMS values for Devices A–C was found to be 2.862 nm 1.867 nm and 1.831 nm, respectively. These results

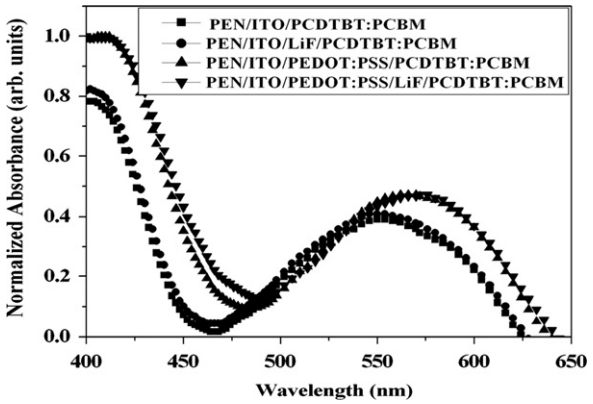

Fig. 2. Intensities of the light absorption spectra of the PCDTBT:PCBM active layers coated on different buffer layers: PEN/ITO/LiF (Device A), PEN/ITO/PEDOT:PSS (Device B), PEN/ITO/PEDOT:PSS/LiF (Device C) and PEN/ITO (without buffer layer) substrates.

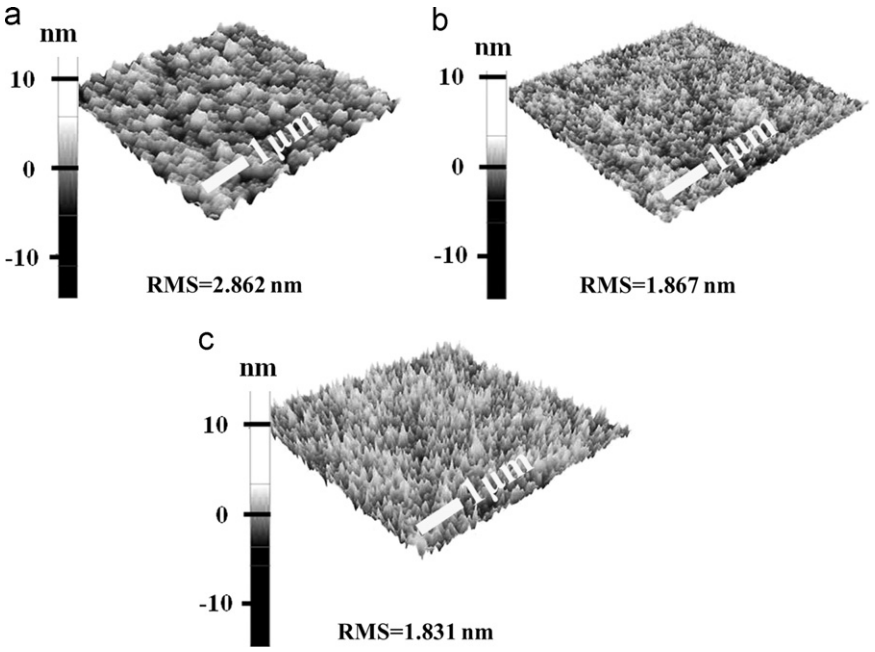

Fig. 3. AFM surface morphologies of (a) Device A (b) Device B and (c) Device C prepared from the different buffer layers.

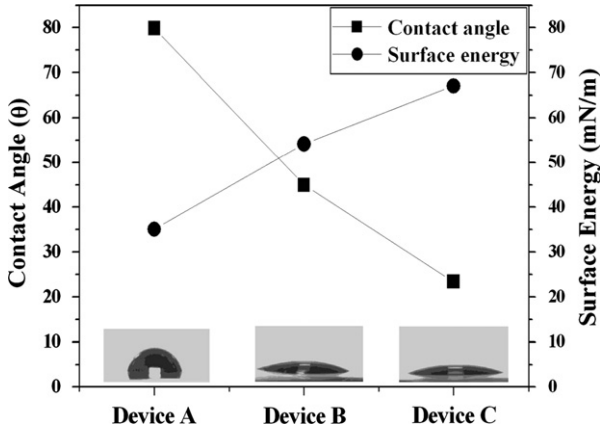

Fig. 4. Wettability images represented by the contact angles (θ) of the D.I. water droplets for Devices A–C.

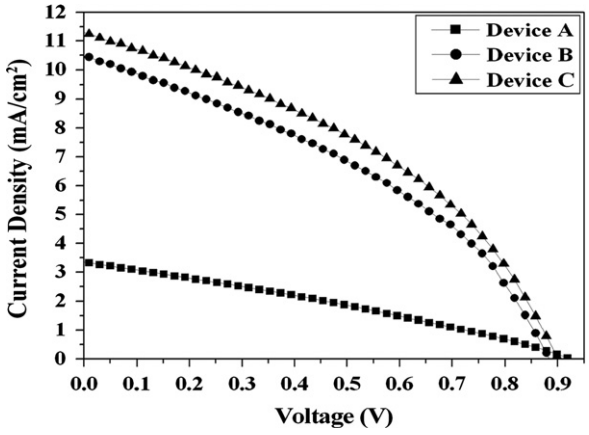

Fig. 5. Current density *versus* voltage (J–V) characteristic curves of the OSCs with PCDTBT:PCBM active layers prepared on the Devices A–C substrates.

indicate that Device A had a coarser film surface morphology compared to Devices B and C, since it shows higher RMS value. This rough active layer film surface results in a poor interfacial adhesion between the buffer layer film and active layer, which leads to a low injection efficiency of the holes into the anode electrode [12].

Fig. 4 shows the wettability images represented by the contact angles (θ) and surface energy (mN/m) for Devices A–C samples. The contact angle had been measured by liquid phase solutions spread on the surface of the buffer film areas. Lower values of θ indicate a better wettability and higher surface energy, as implied by Young's equation [13]. The smallest θ of 23.4° was shown for Device C, which is thought to lead to a good interfacial morphology and adhesion with PCDTBT:PCBM active layer. In contrast, the hydrophobic droplet image with a larger contact angle of $\theta = 79.9°$ was found for Device A (PEN/ITO/LiF substrate).

The surface energy values of the Device A–C were found to be 35.09 mN/m, 54.13 mN/m and 67.09 mN/m, respectively. The Device C exhibited the largest surface energy, which contributes to a good quality buffer layer film. In addition, the improvement of wettability of PCDTBT:PCBM active layer solution was caused mainly by a large surface energy. Therefore, it is important to optimize the surface conditions between the surface energy and morphology of the buffer layers for the improvement of electrical properties.

Fig. 5 shows the current density *versus* voltage (J–V) characteristics and device parameters of the J_{SC}, V_{OC}, fill factor (FF), and the PCE values of the OSCs prepared on

Table 1
J_{SC}, V_{OC}, FF, PCE, R_S and R_P of the flexible OSCs with the PCDTBT:PCBM active layers prepared from the various buffer layers (Devices A–C).

Samples	J_{SC} (mA/cm^2)	V_{OC} (V)	FF (%)	PCE (%)	R_S (KΩ)	R_P (KΩ)
Device A	3.4	0.92	30.0	1.0	3.64	9.0
Device B	10.5	0.88	37.8	3.5	0.76	3.94
Device C	11.4	0.90	39.3	4.0	0.73	4.18

the Device A–C flexible substrates. The maximum J_{SC}, V_{OC}, and FF values were found to be 11.4 mA/cm^2, 0.90 V and 39.3 %, respectively for Device C, indicating that the PCE was calculated to be 4.0%. It has been known that the properties of organic materials are easily degraded by ambient conditions. In this work, the relative low PCE of the flexible OSCs may be caused by the fact that the prepared devices were not subjected to any passivation treatment to protect them against air and moisture. From our experiments, it may be concluded that the observed improvement in the electrical properties of the OSCs coated on the Device C substrate is caused by the enhanced light absorption intensity and smooth film surface morphology as well as the low contact angle and high surface energy of the buffer layer. For Device C, PEDOT:PSS is considered to be a conductive polymer (metal), while LiF and PCDTBT:PCBM are a typical insulator and organic semiconductor, respectively. Therefore, we can discuss the hole injection and transport behaviors for Device C (PEDOT:PSS/LiF/PCDTBT:PCBM system) by using a energy band theory of metal–insulator–semiconductor (MIS) structure. The generated holes in the active layer should have a greater energy than a certain energy level to inject anode electrode side through the insulation potential wall (LiF) by means of the quantum tunneling mechanism [14]. Therefore, Device C with the ITO/PEDOT:PSS/LiF substrate exhibits a high J_{SC}, which is ascribed to improved exporting efficiency of the holes. For an ideal photovoltaic device, a high parallel resistance (R_P) and a low series resistance (R_S) are required [15]. The R_S originates from the ohmic loss in the flexible OSC device, whereas the R_P reflects the degree of leakage current of the device, which relates with the overall quality of the inter layer films. The values of R_S and R_P for Device C are about 0.73 kΩ and 4.18kΩ, respectively. Device C has a lower R_S than other prepared samples, which is responsible for the increase of J_{SC} due to the formation of a better ohmic contact.

The J_{SC}, V_{OC}, FF, PCE, R_S and R_P values of the flexible OSCs with the PCDTBT:PCBM active layers prepared from the various buffer layers (Devices A–C) are summarized in Table 1.

4. Conclusions

We fabricated the flexible organic solar cells (OSCs) using a PCDTBT and PCBM active layer as the electron donor and acceptor materials, respectively. The active layer was spin-coated onto three different buffer layers such as PEN / ITO/LiF (Device A), PEN/ITO/PEDOT:PSS (Device B), and PEN/ITO/PEDOT:PSS/LiF (Device C). The effects of buffer layers on the properties of devices were investigated. The performance of the flexible OSC coated on the Device C substrate was superior to the other prepared samples (Devices A and B), showing the maximum J_{SC}, V_{OC}, FF, and PCE values were about 11.4 mA/cm^2, 0.90 V, 39.3% and 4.0%, respectively. From the AFM measurement and contact angle images, the improved electrical properties may be attributed to a smooth film surface as well as a good wettability with a lower contact angle and higher surface energy of the buffer film layer.

Acknowledgements

This work was supported by The National Research Foundation of Korea (NRF) grant funded by The Korea government (MEST) (2011-0015835).

References

[1] G. Yu, J. Gao, J.C. Hemmelen, F. Wudl, A.J. Heeger, Polymer photovoltaic cells: enhanced efficiencies via a network of internal donor–acceptor heterojunctions, Science 270 (1995) 1789–1791.
[2] F.C. Krebs, H. Spanggard, T. Kjaer, M. Biancardo, J. Alstrup, Large area plastic solar cell modules, Materials Science and Engineering B 138 (2007) 106–111.
[3] L. Blankenburg, K. Schultheis, H. Schache, S. Sensfuss, M. Schrodner, Reel-to-reel wet coating as an efficient up-scaling technique for the production of bulk-heterojunction polymer solar cells, Solar Energy Materials and Solar Cells 93 (2009) 476–483.
[4] M. Niggemann, B. Zimmermann, J. Haschke, M. Glatthaar, A. Gombert, Organic solar cell modules for specific applications-form energy autonomous systems to large area photovoltaics, Thin Solid Films 516 (2008) 7181–7187.
[5] G. Li, C.W. Chu, V. Shrotriya, J. Huang, Y. Yang, Efficient inverted polymer solar cells, Applied Physics Letters 88 (2006) 253503-1–253503-3.
[6] J.Y. Kim, S.H. Kim, H.H. Lee, K. Lee, W. Ma, X. Gong, A.J. Heeger, New architecture for high-efficiency polymer photovolataic cells using solution-based titanium oxide as an optical spacer, Advanced Materials 18 (2006) 572–576.
[7] R.F. Service, Outlook brightens for plastic solar cells, Science 332 (2011) 293.
[8] C.J. Bradec, Organic photovoltaics: technology and market, Solar Energy Materials and Solar Cells 83 (2004) 273–292.
[9] C. Walduf, P. Schilinsky, J. Hauch, C.J. Bradec, Material and device concepts for organic photovoltaics: towards competitive efficiencies, Thin Solid Films 451–452 (2004) 503–507.
[10] C.J. Brabec, S.E. Shaheen, C. Winder, N.S. Sariciftci, P. Denk, Effect of LiF/metal electrodes on the performance of plastic solar cells, Applied Physics Letters 80 (2002) 1288–1290.

[11] F. Liu, S. Shao, X. Guo, Y. Zhao, Z. Xie, Efficient polymer photovoltaic cells using solution-processed MoO_3 as anode buffer layer, Solar Energy Materials and Solar Cells 94 (2010) 842–845.
[12] H.Y. Chen, J. Hou, S. Zhang, Y. Liang, G. Yang, Y. Yang, L. Yu, Y. Wu, G. Li, Polymer solar cells with enhanced open-circuit voltage and efficiency, Nature Photonics 3 (2009) 649–653.
[13] G.–H. Kim, H.–K. Song, J.Y. Kim, The effect of introducing a buffer layer to polymer solar cells on cell efficiency, Solar Energy Materials and Solar Cells 95 (2011) 1119.
[14] X. Xi, Q. Meng, F. Li, Y. Ding, J. Ji, Z. Shi, G. Li, The characteristics of the small molecule organic solar cells with PEDOT:PSS/LiF double anode buffer layer system, Solar Energy Materials and Solar Cells 94 (2010) 623–628.
[15] J. Xue, S. Uchida, B.P. Rand, S.R. Forrest, Organic small molecule solar cells with a homogeneously mixed CuPc:C_{60} active layer, Applied Physics Letters 84 (2004) 3013–3015.